ISSN 0036-0236, Russian Journal of Inorganic Chemistry, 2016, Vol. 61, No. 6, pp. 667–673. © Pleiades Publishing, Ltd., 2016.
Original Russian Text © N.P. Simonenko, E.P. Simonenko, V.G. Sevastyanov, N.T. Kuznetsov, 2016, published in Zhurnal Neorganicheskoi Khimii, 2016, Vol. 61, No. 6, pp. 703–709.

SYNTHESIS AND PROPERTIES OF INORGANIC COMPOUNDS

Preparation of Nanostructured Thin Films of Yttrium Aluminum Garnet ($Y_3Al_5O_{12}$) by Sol–Gel Technology

N. P. Simonenko, E. P. Simonenko, V. G. Sevastyanov, and N. T. Kuznetsov

Kurnakov Institute of General and Inorganic Chemistry, Russian Academy of Sciences, Leninskii pr. 31, Moscow, 119991 Russia

e-mail: n_simonenko@mail.ru

Received November 24, 2015

Abstract—The synthesis of hydrolytically active heteroligand coordination compounds $[M(C_5H_7O_2)_{3-x}(C_5H_{11}O^i)_x]$ (where $M = Al^{3+}$ and Y^{3+}) using aluminum and yttrium acetylacetonates has been studied. The gel formation kinetics in their solutions upon hydrolysis and polycondensation has also been studied. Thin films of a solution of these precursors have been applied to polished sapphire substrates by dip coating. The crystallization of nanostructured yttrium aluminum garnet ($Y_3Al_5O_{12}$) films during heat treatment of xerogel coatings under various conditions has been studied. How the phase composition, microstructure, and particle size depend on the synthesis parameters has been recognized.

DOI: 10.1134/S003602361606019X

The rapid growth of industries in the world makes the design of new materials that would satisfy contemporary performance requirements increasingly topical. In the field of electronics and optics, for example, the production of thin film materials of complex composition, specifically that comprise yttrium aluminum garnet ($Y_3Al_5O_{12}$), becomes topical. The scientific community pays much attention to studies into autolocated excitons, luminescence, and photoelectron emission in the context of a potential scintillation use of similar films produced by liquid-phase epitaxy [1–4]. Cerium-doped yttrium aluminum garnet can also be deposited as coatings by sedimentation [5]; in some cases, particles are coated with silica for enhancing luminescence [6]. Rare-earth dopants such as terbium, europium, and neodymium are also used, and coatings are applied by pulsed laser deposition or sol–gel technology using alkoxides, acetates, and inorganic salts of metals [7–10]. In spite of the merits of the above-described methods, there is now need in new technologies that would make it possible to tailor the characteristics of the films such as thickness, phase composition, and microstructure. One such strategy is sol–gel technology where the precursors are hydrolytically active heteroligand complexes $[M(C_5H_7O_2)_x(OR)_y]$, which are prepared via controlled partial destructive substitution of alkoxy moieties for β-diketonate ligands. An alteration of composition in the coordination sphere of the precursor determines its reactivity and, accordingly, the kinetics of rheology of its solutions upon hydrolysis and polycondensation, which is of special importance for thin film formation. This strategy makes it possible to prepare both highly disperse metal oxides in powders [11–13], thin nanostructured films [14, 15], microtubes [16], or composite matrices [17], and refractory carbides [18–20].

Therefore, our study was directed to the specifics of synthesis of hydrolytically active heteroligand complexes $[M(C_5H_7O_2)_{3-x}(C_5H_{11}O^i)_x]$ (where $M = Al^{3+}$ and Y^{3+}) and to use them in the manufacture of thin nanostructured films of yttrium aluminum garnet ($Y_3Al_5O_{12}$) on sapphire substrates.

EXPERIMENTAL

Metal acetylacetonates were prepared from $Y(NO_3)_3 \cdot 6H_2O$ (chemically pure grade), $Al(NO_3)_3 \cdot 9H_2O$ (pure grade), $C_5H_8O_2$ (pure), and 5% aqueous solution of $NH_3 \cdot H_2O$ (high purity grade). The solvent used for the prepared chelates and the source of alkoxy groups in the synthesis of heteroligand complexes was isoamyl alcohol $^iC_5H_{11}OH$ (pure for analysis grade).

The precursors $[M(C_5H_7O_2)_{3-x}(C_5H_{11}O^i)_x]$ (where $M = Al^{3+}$ and Y^{3+}) were prepared by the heat treatment of a solution of aluminum and yttrium acetylacetonates in isoamyl alcohol in a round-bottomed flask equipped with a refluxer on a sand bath.

Films of solution of heteroligand complexes were applied to polished polycrystalline sapphire substrates by the dip-coating method.

Electronic (UV–Vis) spectra of solutions of coordination compounds before and after $C_5H_7O_2$ ligands were substituted were recorded on an SF-56 UV–Vis

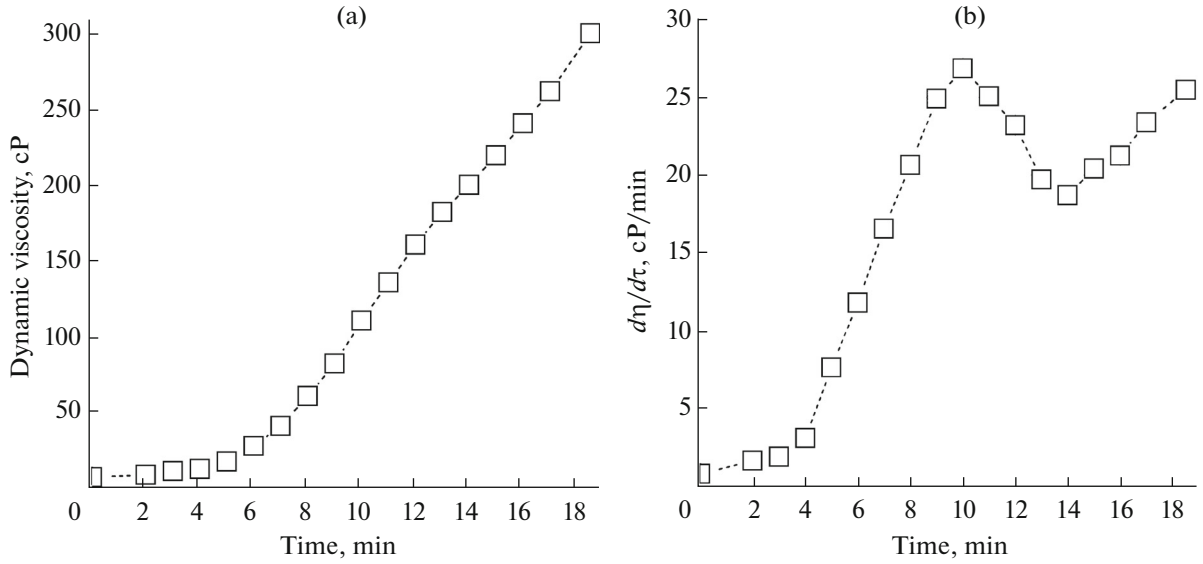

Fig. 1. (a) Dynamic viscosity of solution of aluminum and yttrium alkoxyacetylacetonates during hydrolysis and (b) its derivative curve.

spectrophotometer once the solutions were diluted with butanol (to $c = 4 \times 10^{-4}$ mol/L).

IR transmission spectra of solutions before and after $C_5H_7O_2$ ligands were substituted were recorded on an FT-08 Infralum FT-IR spectrometer (KBr glasses; wavenumber window: 350–4000 cm^{-1}). For recording IR reflection spectra of oxide films, a PIKE EasiDiff diffuse reflection unit was used.

The evolution of rheology of the solution of heteroligand precursor during hydrolysis and polycondensation was studied with a Fungilab Smart L rotational viscometer (shear speed: 100 rpm; L2 spindle; temperature: 22 ± 2°C).

X-ray diffraction patterns from the surface of oxide films were recorded on a D8 Advance (Bruker) X-ray diffractometer in the range 28°–35° 2θ with 0.02° resolution and a signal accumulation time per point of 2 s.

The microstructure of oxide films was studied with an NVision 40 (Carl Zeiss) three-beam workstation equipped with an EDX Oxford Instruments energy-dispersive analysis unit, and with a Solver Pro-M scanning probe microscope.

The adhesion of films was studied by a standard V-notch test using an Elcometer 107 adhesion meter.

RESULTS AND DISCUSSION

Synthesis of Heteroligand Precursors

A solution of the as-synthesized complexes $[Y(C_5H_7O_2)_3]$ and $[Al(C_5H_7O_2)_3]$ in isoamyl alcohol with the metal ratio set by the stoichiometry of the target oxide $Y_3Al_5O_{12}$, was prepared in a round-bottomed flask equipped with a refluxer. The solution was heat treated at the boiling temperature (131 ± 2°C) on a sand bath for 5 h (the total metal concentration was 0.2 mol/L). As a result, there was partial destructive substitution of $C_5H_{11}O^i$ groups for $C_5H_7O_2$ ligands, which was verified by a reduction in intensity of IR absorption bands of the solution in the range 1500–1700 cm^{-1} (these bands relate to the stretching vibrations of C=C and C=O in coordinated chelate moieties) and the appearance of a new double absorption band in the range 1700–1760 cm^{-1} (this band arises from the ν(C=O) mode of side reaction products, namely acetone and ester). In the UV–Vis spectrum of the solution of heteroligand precursors diluted to a metal concentration of 4×10^{-4} mol/L, absorption bands were also reduced in intensity in the range 250–320 nm (this range is characteristic of coordinated acetylacetonate ligands). The degree of substitution of alkoxy moieties for $C_5H_7O_2$ groups was 93% as estimated from the Bouguer–Lambert–Beer law.

How the rheology of the solution of heteroligand precursors changed upon hydrolysis and polycondensation was studied by rotational viscometry. Addition of a hydrolyzing component (ethanolic solution of water: 0.42 mL, $\varphi(H_2O) = 0.3$) to the solution of $[M(C_5H_7O_2)_{3-x}(C_5H_{11}O^i)_x]$ (14 mL) induced hydrolysis and subsequent polycondensation, with an attendant increase in dynamic viscosity over time and the formation of a transparent gel (Fig. 1). Figure 1 makes it clear that the dynamic viscosity of the sys-

tem increased by a factor of more than 40 (from 7 to 300 cP) in 18.5 min, and the derivative curve in this figure shows that the peak gel formation rate, equal to 27 cP/min, was attained in 10 min since the hydrolysis was initiated. The run of the derivative curve also manifests the two-step character of the process, whose rate decreases in the range 10–14 min (to 19 cP) and then increases again. Thus, the heteroligand precursors synthesized are shown to actively react with water with an attendant strong change in rheology of their solutions, and this should be taken into account in the manufacture of thin films of tailored thickness and tailored microstructure.

Application of Thin Films of Precursor Solutions to Polished Sapphire Substrates

As we showed earlier [15], when a thin film of a solution of heteroligand complexes $[M(C_5H_7O_2)_{3-x}(C_5H_{11}O)_x]$ is applied to the substrate surface at 22°C, acetone and ester are consecutively evaporated from the film bulk (in 5 min), followed by the isoamyl alcohol solvent (in 30 min). The hydrolysis of the precursor by atmospheric moisture ends in 60 min. Relying on these results, we coated the surface of polished polycrystalline sapphire substrates with a thin film of the as-prepared solution of aluminum and yttrium alkoxyacetylacetonates by dip coating (withdrawal rate: 1 mm/s); afterwards, the samples were kept in air for 60 min for the completion of formation of a thin xerogel film.

Crystallization of $Y_3Al_5O_{12}$ Thin Films

The sapphire substrate samples coated with thin xerogel films were then heat-treated under various conditions in order to study the crystallization of yttrium aluminum garnet.

Heating was performed to 800, 1000, and 1200°C at a rate of ~20 K/min without exposure and was followed by cooling. The surfaces of the thus-prepared films were then studied by IR spectroscopy. The IR reflection spectra (Fig. 2) show strong absorption bands characteristic of yttrium aluminum garnet that appeared after the xerogel film was heated above 1000°C.

The results of X-ray powder diffraction analysis of the surface of samples (Fig. 3) imply that the oxide film remains X-ray amorphous at 800°C. Heating of the xerogel coating to 1000°C results in the crystallization of the target cubic phase (yttrium aluminum garnet) with an average crystallite size of 25 nm. The X-ray diffraction pattern also features a reflection from the orthorhombic phase of $YAlO_3$. When temperature rises further to 1200°C, a single-phase $Y_3Al_5O_{12}$ film is formed with an average crystallite size of 40 nm, which agrees well with the results of IR spectroscopy. Thus, we may assume that, in our case, a rise

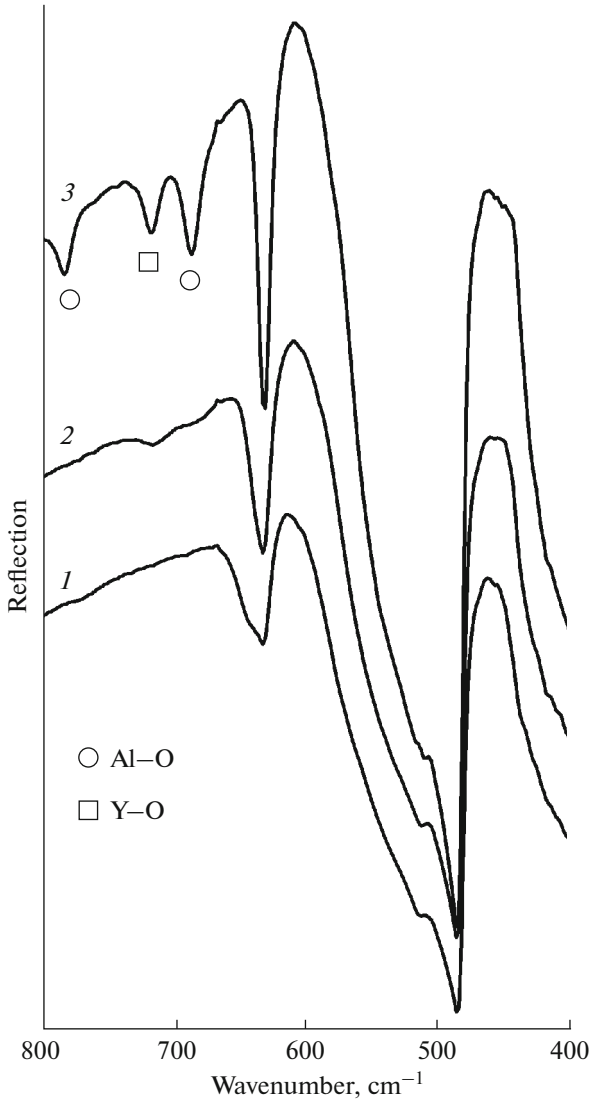

Fig. 2. IR reflection spectra of $Y_3Al_5O_{12}$ films on sapphire substrates prepared at (*1*) 800, (*2*) 1000, and (*3*) 1200°C.

in temperature from 800 to 1200°C causes the consecutive crystallization of a highly disperse oxide film: $YAlO_3 \rightarrow Y_3Al_5O_{12}$.

From the results of microstructure analysis by scanning electron microscopy (SEM), we may infer that coatings become more textured and more porous as temperature rises (Fig. 4). For the yttrium aluminum garnet film prepared at 1200°C, we observe self-organization of elongated particles (200–300 nm long, ~100 nm in diameter), likely, in the direction of crystallization centers, which are at distances of 3–5 μm from one another. Microscopy also helped us to determine the factors that are responsible for the appearance of damages in coatings. The micrographs show

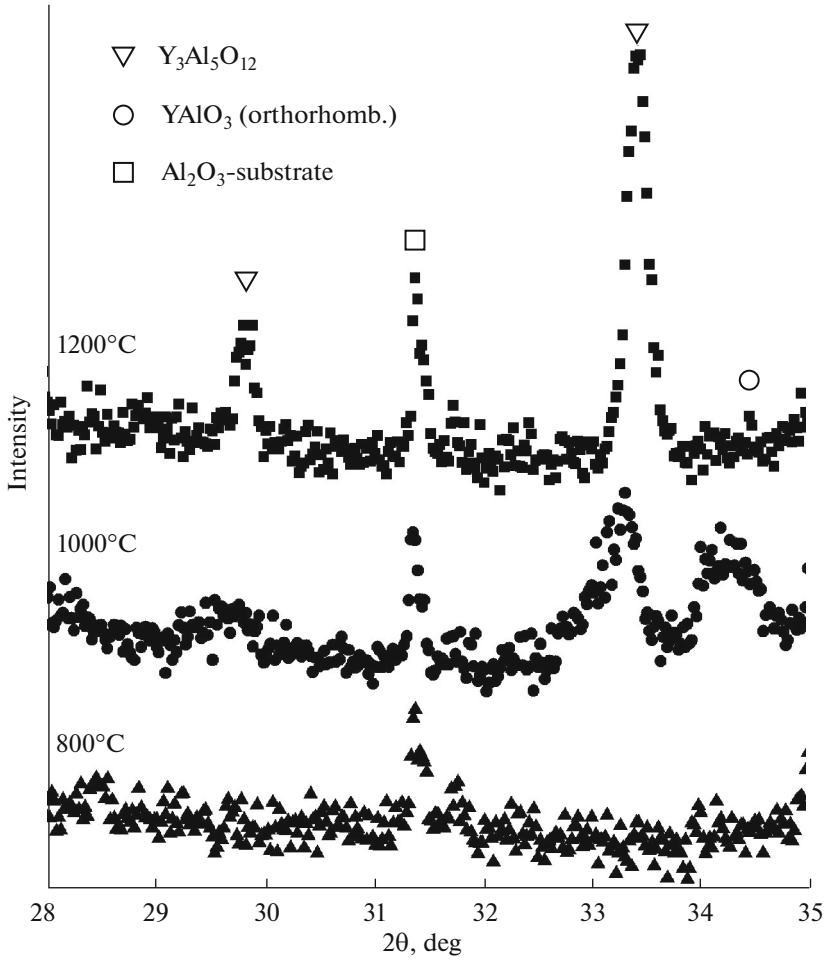

Fig. 3. X-ray diffraction patterns of $Y_3Al_5O_{12}$ films prepared at various temperatures.

that, regardless of heat-treatment parameters, film exfoliation in some regions is caused by an excessive thickness of the precursor solution layer (>200 nm). Further, defects with large height difference on the substrate surface also result in coating breaks because of locally uncompensated surface tension at the syneresis stage of the gel film.

The energy dispersive elemental analysis of surface microregions of the films verified the set metal ratio and the formation of the oxide $Y_3Al_5O_{12}$.

The results of scanning probe microscopy (SPM) support the character of film microstructure derived from SEM images. The average size of constituent particles of the coating increases from 30 to 50 nm as temperature rises from 800 to 1000°C; the maximal height difference across the 25 μm^2 surface area increases from 14 to 18 nm (Fig. 5). The ordered microstructure of the yttrium aluminum garnet film formed at 1200°C is also verified by this method: particles of elongated shapes are directed toward crystallization centers, and the maximal height difference across the 25 μm^2 surface area is 60 nm. The regions of directional organization of particles have sizes of ~3 μm, and there are rather distinct boundaries between them. The separation between crystallization centers is 3–5 μm (Fig. 6), as by SEM data.

The adhesion of oxide films was evaluated by a standard V-notch test. The nanostructured coatings were found to refer to maximal adhesion classes of the ISO (0) and ASTM (5B) international standards, and the coating technology may be recommended to the manufacturers of relevant structures.

Thus, we have studied the synthesis specifics of hydrolytically active heteroligand coordination compounds $[M(C_5H_7O_2)_{3-x}(C_5H_{11}O^i)_x]$ (where M = Al^{3+} and Y^{3+}) with a ~93% degree of substitution of alkoxy moieties for chelating ligands, and studied the gel-formation kinetics of their solutions upon hydrolysis and polycondensation. We have used the precursor solu-

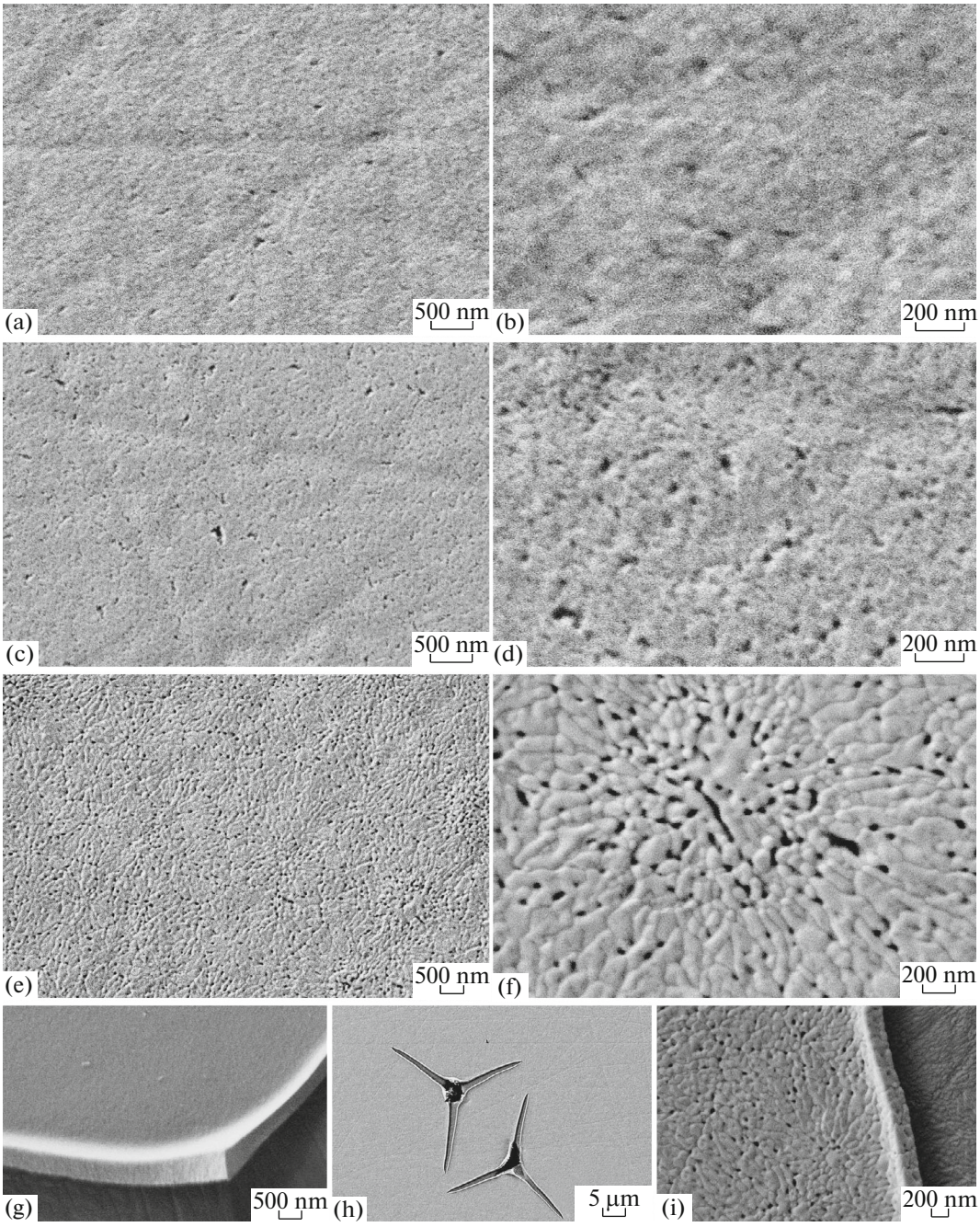

Fig. 4. Microstructure of $Y_3Al_5O_{12}$ films prepared at (a, b) 800, (c, d) 1000, and (e, f) 1200°C; defects are exfoliations and breaks at (g) 800, (h) 1000, and (i) 1200°C (SEM).

tion to apply nanostructured thin films of yttrium aluminum garnet to sapphire substrates using the dip coating method. Heating of the xerogel coating from 800 to 1200°C has been found to induce consecutive crystallization of a highly disperse oxide film: $YAlO_3 \rightarrow Y_3Al_5O_{12}$. Heating to 1200°C gives rise to the self-organization of a single-phase nanocrystalline thin $Y_3Al_5O_{12}$ film that consists of elongated particles (200–300 nm long, ~100 nm in diameter) ordered in the direction of crystallization centers, which are separated at 3–5 μm from each other.

Scanning probe microscopy helped us to discover that the roughness of $Y_3Al_5O_{12}$ films increases from 14 to 60 nm as the synthesis temperature rises; the films

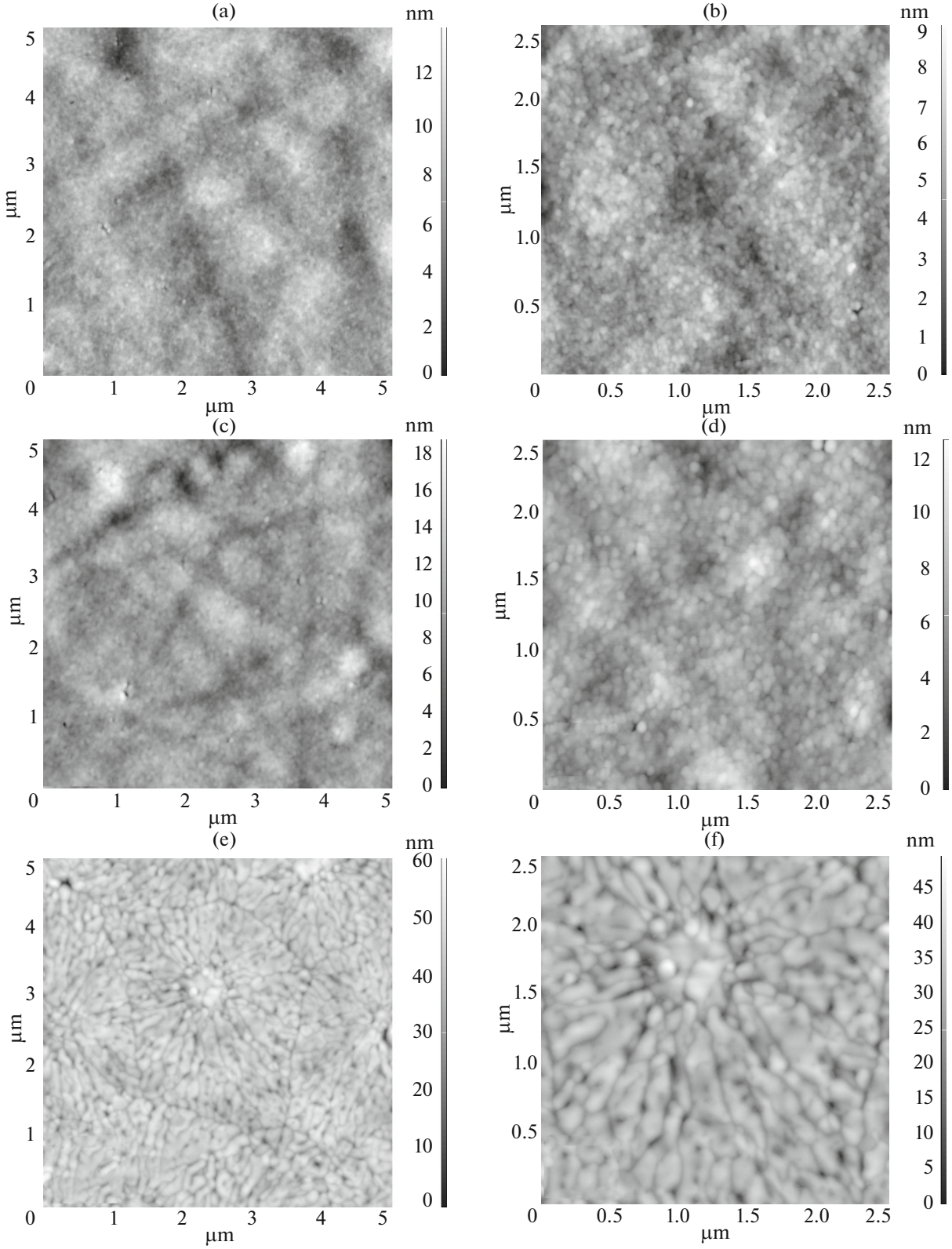

Fig. 5. Microstructure of $Y_3Al_5O_{12}$ films prepared at (a, b) 800, (c, d) 1000, and (e, f) 1200°C (SPM).

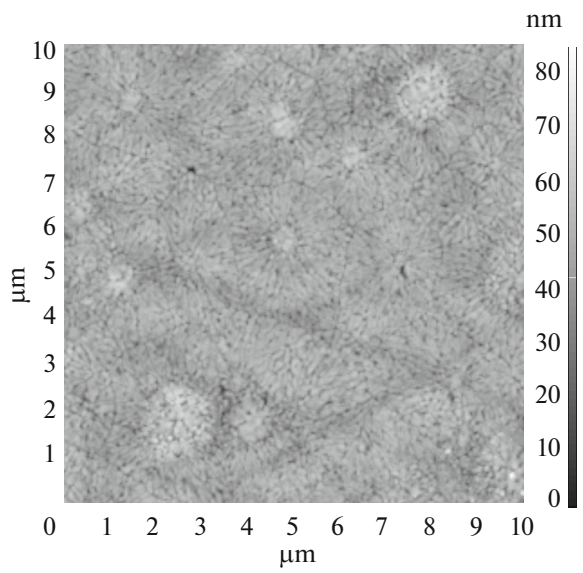

Fig. 6. Ordered microstructure of a $Y_3Al_5O_{12}$ film prepared at 1200°C (SPM).

have the maximal adhesion classes according to international standards: ISO (0) and ASTM (5B).

ACKNOWLEDGMENTS

This study was supported by the Russian Foundation for Basic Research (project nos. 14-03-00983 A, 15-03-07568 A, 14-03-31002 mol_a, and 15-29-01213 ofi_m) and by a grant from the President of the Russian Federation (grant no. MK-4140.2015.3).

REFERENCES

1. Yu. Zorenko, A. Voloshinovskii, V. Savchyn, et al., Phys. Stat. Solidi B **244**, 2180 (2007).
2. V. Babin, V. Bichevin, V. Gorbenko, et al., Phys. Stat. Solidi B **246**, 1318 (2009).
3. M. Kucera, K. Nitsch, M. Nikl, et al., J. Cryst. Growth **312**, 1538 (2010).
4. P. Prusa, M. Nikl, J. A. Mares, et al., Phys. Stat. Solidi A **206**, 1494 (2009).
5. J. R. Oh, S. -H. Cho, Y. -H. Lee, et al., Optics Express **17**, 7450 (2009).
6. Y.-T. Nien, K.-M. Chen, and I.-G. Chen, J. Am. Ceram. Soc. **93**, 1688 (2010).
7. A. Potdevin, G. Chadeyron, D. Boyer, et al., J. Phys. D: Appl. Phys. **38**, 3251 (2005).
8. P. Prusa, M. Nikl, J. A. Mares, et al., Phys. Stat. Solidi A **206**, 1494 (2009).
9. J. Sonsky, M. Jelínek, P. Hríbek, et al., Laser Phys. **8**, 285 (1998).
10. G. A. Hirata, O. A. Lopez, L. E. Shea, et al., J. Vac. Sci. Technol., A **14**, 1694 (1996).
11. N. T. Kuznetsov, V. G. Sevast'yanov, E. P. Simonenko, et al., RU Patent No. 2407705 (2010).
12. V. G. Sevast'yanov, E. P. Simonenko, N. P. Simonenko, et al., Russ. J. Inorg. Chem. **57**, 307 (2012). doi 10.1134/S0036023612030278
13. E. P. Simonenko, N. P. Simonenko, V. G. Sevastyanov, et al., Russ. J. Inorg. Chem. **57**, 1521 (2012). doi 10.1134/S0036023612120194
14. N. T. Kuznetsov, V. G. Sevast'yanov, E. P. Simonenko, et al., RU Patent No. 2521643 (2014)
15. N. P. Simonenko, E. P. Simonenko, V. G. Sevastyanov, et al., Russ. J. Inorg. Chem. **60**, 795 (2015).
16. N. P. Simonenko, E. P. Simonenko, V. G. Sevast'yanov, et al., Yad. Fiz. Inzh. **5**, 331 (2014).
17. E. P. Simonenko, N. P. Simonenko, V. G. Sevastyanov, et al., Compos. Nanostruct., No. 4, 52 (2011).
18. V. G. Sevastyanov, E. P. Simonenko, N. A. Ignatov, et al., Russ. J. Inorg. Chem. **56**, 661 (2011). doi 10.1134/S0036023611050214
19. E. P. Simonenko, N. A. Ignatov, N. P. Simonenko, et al., Russ. J. Inorg. Chem. **56**, 1681 (2011). doi 10.1134/S0036023611110258
20. N. T. Kuznetsov, V. G. Sevastyanov, E. P. Simonenko, et al., RU Patent No. 2333888 (2008).

Translated by O. Fedorova